doi:10.2533/chimia.2022.354 Chimia 76 (2022) 354–360

The Separation Power of Highly Porous 3D Nanofiber Sponges

Patricia Risch[§ab] and Christian Adlhart*[a]

[§]SCS-DSM Award for the best virtual poster in Polymers, Colloids & Interfaces

Abstract: Sponges formed by the self-assembly of nanofiber building blocks are versatile materials used in various fields such as filtration, thermal insulation, scaffolding or sound absorption. Their potential seems to be constantly expanding given the variety of possible fiber materials, from bio-based to fossil polymers to inorganic nanofibers. In general, nanofiber sponges – also called nanofiber aerogels – are flexible, have low density, and a large specific surface area thanks to their tunable open-porous nanofiber based architecture. The latter property makes nanofiber sponges an interesting material for separation problems, as recently demonstrated for a variety of mixtures such as aerosols, emulsions, dispersions, solutions or two-phase systems. Due to their highly porous structure, they generally exhibit high filtration efficiency, flow rate and capacity. This article reviews the state of the art in the application of 3D nanofiber sponges for the different classes of mixtures. We will discuss on a mechanistic basis why nanofiber sponges are particularly well suited for separation applications. Finally, their performance in terms of efficiency, flow rate, capacity and regeneration will be compared to other fiber-based filter media.

Keywords: Aerosol filtration · Filtration mechanisms · Microplastics · Nanofiber aerogels · Nanofiber sponges · Water purification

Patricia Risch completed her bachelor's degree in chemistry with a specialization in biological chemistry at the Zurich University of Applied Sciences (ZHAW) in 2019. She then moved to the Center for Functional Materials and Nanotechnology of Prof. Dr. Christian Adlhart as a research associate to continue her research on the synthesis of nanofiber sponges for the filtration of microplastics. She is currently working at Avelo AG on the development of a breath aerosol diagnostic test for the detection of respiratory infections.

Introduction

The separation of mixtures such as aerosols, emulsions, dispersions or solutions is an important step in many industrial and environmental processes.[1] Separation by filtration and related techniques is achieved by placing a permeable filter in the path of the flowing mixture. This allows the passage of the purified/clarified gas or liquid while acting as a barrier to the suspended/dissolved particles or solutes. Inherent performance issues are the interaction between the permeable filter and the solutes, clogging, adsorption capacity, and regeneration.[1] Recent examples show[2] that 3D nanofiber sponges have the potential to outperform their widely used counterparts, which are the essentially 2D nanofiber mats or membranes. In particular, the limitations of densely packed nanofiber mats in terms of low flow rate and low capacity are overcome by the highly porous nanofiber sponges. Fig. 1 shows a chitosan nanofiber sponge with its inherent properties such as fiber-based, open porous, lightweight, elastic, flexible, mechanically stable, and with a large surface area. The porosity is required for efficient mass transfer and low pressure drop, while the nanofiber-based architecture enables a large specific surface area. Therefore, nanofiber sponges are excellent candidates for filtration and separation applications.

The preparation, functionalization, and application of nanofiber sponges have recently been described in several review articles.[2,3] In general, nanofiber sponges are prepared from nanofibers (Fig. 2a,b), which are usually obtained by electrospinning (Fig. 2c). The main physical principle is shown in Fig. 2d, where suspensions of short nanofibers are frozen while the self-assembly of nanofiber building blocks is initiated. This self-assembly process of nanofiber sponges is fundamentally different from classical aerogels, where the molecular building blocks form a colloid during a gelation process in the liquid phase[4] (nevertheless, the misleading term nanofiber aerogel is often used instead of nanofiber sponge). The frozen suspension medium is then removed by sublimation to prevent collapse of the nanofiber construct. Final stability is usually achieved by strengthening the weak fiber junctions. Post-treatment processes such as thermal treatment,[5] chemical cross-linking,[6] solvent vapor welding[7] or chemical vapor deposition[8] are used for this purpose. Figs 2e and f show the low bulk density and potential size of nanofiber sponges. In terms of size, nanofiber sponges are multiscale hierarchical objects covering seven orders of magnitude from 50 nm nanofiber building blocks to 50 cm-sized workpieces (Fig. 2g). The most interesting aspect of these highly porous materials in terms of filtration is the different dimensions of the pores. The major pores (Figs 2h–k) are formed by the growing crystals of the suspension liquid, and the size of these major pores can be tuned between 10 and 150 µm by precisely controlling the freezing process.[9] Minor pores between 1 and 5 µm (Fig. 2l) are formed by the network of tangled nanofibers trapped between the growing crystals. The size and distribution of the minor and major pores have an enormous influence on the mass transfer and separa-

*Correspondence: Prof. Dr. C. Adlhart, E-mail: christian.adlhart@zhaw.ch

[a]Institute of Chemistry and Biotechnology, Zurich University of Applied Sciences ZHAW, CH-8820 Wädenswil, Switzerland; [b]Avelo AG, Rütistrasse 16, 8952 Schlieren, Switzerland.

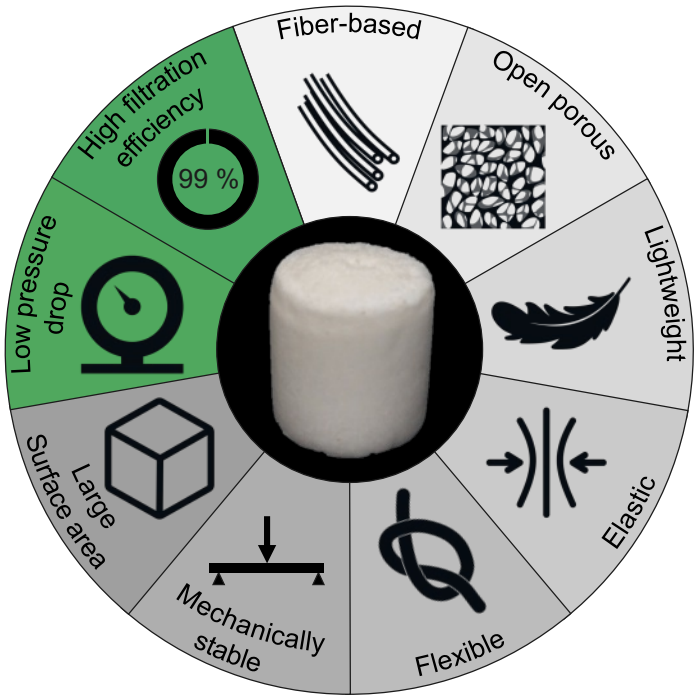

Fig. 1. Characteristic properties of nanofiber sponges.

tion properties of the mixture to be filtered. This applies to separation problems in the gas phase (aerosols) as well as in the liquid phase (emulsions, dispersions, solutions or two-phase systems).

Filtration of Aerosols

Aerosols are dynamic suspensions of solid or liquid particles in a gas. They are of natural or anthropogenic origin. Because they are of concern to the environment (*e.g.* cloud formation), technology (*e.g.* cleanrooms), or health (*e.g.* viruses), they require filtration solutions. The mechanism of single fiber filtration (Fig. 3a) of aerosols is well understood and can be described as the sum of several physical interactions. While diffusion dominates for small particles <0.2 µm such as viruses, larger particles of about 0.5 µm act by interception or direct impact (inertia >1.0 µm).[2,11] Filters consisting essentially of 2D nanofiber mats show lower performance at higher airflows due to lower diffusion interaction and limited filtration capacity due to formation of a filter cake (= growing layer of aerosols deposited on the filter surface).[5] Both factors are overcome with the porous 3D nanofiber sponges. On the one hand, the long interaction path allows sufficient diffusion interaction even at high airflow, and on the other hand, aerosols are mainly deposited in deeper regions of the sponge without forming a significant filter cake.[5] Recent examples are listed in Table 1. Although the filtration performance of the materials cannot be directly compared because the selected experimental conditions such as particle size and face velocity directly affect the pressure drop and filtration efficiency, a remarkable efficiency of >99% is observed for most filters, reaching up to 99.998%.[5] However, in the latter case, the differential pressure was 550 Pa. This is more than the limit of 70 Pa for the widely used FFP2 filter masks. But the allowable leakage of FFP2 filters is 3000 times higher (6% compared to the 0.002% achieved here).[12] The high filtration efficiency for particles much smaller than the pores of nanofiber sponges is not due to a sieving effect. It is mainly achieved by the long residence time of the aerosol within the 3D filter medium. This enables efficient diffusion-based adsorption even at high face velocity, while the adsorption efficiency of comparable 2D nanofiber mats decreases significantly with increasing face velocity.[5] Several studies have demonstrated long-term filtration performance without significant performance degradation for 40 h[13] or for >1 g m^{-2} deposited particles.[5] This is due to the high porosity of these materials. Qiao *et al.* also investigated the potential of regeneration by washing with ethanol, which was successful for 5 cycles.[14] 2D nanofiber mats, on the other hand, are more sensitive to surface deposition,[5] but in-process regeneration strategies such as reverse pulse cleaning have been developed to extend their lifetime.[15] Remarkably, nanofiber sponge filters are not limited to a single class of materials, but have been fabricated from synthetic polymers such as PI,[6,7,16] PVA-*co*-PE,[17] or PAN,[13] blends with biopolymers such as Pul/PVA[3a,5] or pure biopolymers such as silk fibroin[18] or cellulose.[19] While electrospinning is the predominant technology used to produce nanofibers, some fibers were isolated from cellulose pulp (cellulose nanofibers[20]) or obtained by melt extrusion with phase separation (PVA-*co*-PE[17]). The effect of surface modification on filtration efficiency is small,[13] but sometimes necessary to achieve mechanical stability or moisture stability. However, it has been shown that antiviral and antibacterial properties can be achieved with a reduction of 6 log PFU and CFU by a regenerable N-halamine finish.[19a]

Filtration of Emulsions

Emulsions are liquid-in-liquid mixtures such as homogenized milk, an oil-in-water (O/W) emulsion. In the processing industries, such as petrochemical, metallurgical, or food processing, large amounts of liquid waste are generated in the form of O/W or W/O emulsions. Therefore, demulsification is a critical process in these industries.[21] The use of porous media can be an efficient method for separating emulsions. When the pore size is larger than the droplet size, the mechanism is based on coalescence separation rather than size separation:[22] emulsified droplets making their way through the sponge deposit on the fiber, the collision of adjacent droplets ruptures the water-oil interface, and the droplets fuse to form larger droplets.[23] A superhydrophobic fiber surface is required for the separation of W/O emulsions, *e.g.* PAN fibers coated with SiO_2 nanoparticles (NP)[22] or polyimide fibers coated with silane,[24] while hydrophilic nanofibrillated cellulose fibers are suitable for the separation of O/W emulsions, *e.g.* oil in seawater.[25] Li *et al.* demonstrated tunable wettability for sponges made from phenolic resin-based fibers obtained by a hydrothermal process and rendered hydrophobic by thermal treatment.[26] Both O/W and W/O emulsions were successfully separated. The reported separation efficiencies ranged from 94 to 99.995%, and thanks to the porous sponge structure, the filtration flux ranged from 250 to 1.8×10^5 l m^{-2} h^{-1}. Once the capacity of the sponges was reached by coalesced droplets entrapped in their pores, the original flux and separation efficiency were easily restored, *e.g.* by washing with ethanol[22] or squeezing and drying.[24,26] Table 2 gives an overview of recent achievements in the field of emulsion filtration and shows the wide applicability of nanofiber sponges for such separation tasks.

Filtration of Suspensions

The dominant mechanisms for filtration of particles >0.5 µm from liquids are direct sieving and interception.[1] When suspended particles are deposited on the surface of the filter media, a filter cake is formed by a bridging mechanism. This growing layer of retained particles on the surface of the filter media prevents clogging of its pores. Therefore, filter aids such as diatomaceous earth are often added to form the filter cake. However, not every filtration results in the formation of a filter cake, as shown in Fig. 3c. In constant pressure filtration, the different types of filtration can be expressed by a common differential equation (Eqn. (1)):

$$\frac{d^2t}{dV^2} = k_n \cdot \left(\frac{dt}{dV}\right)^n \quad (1)$$

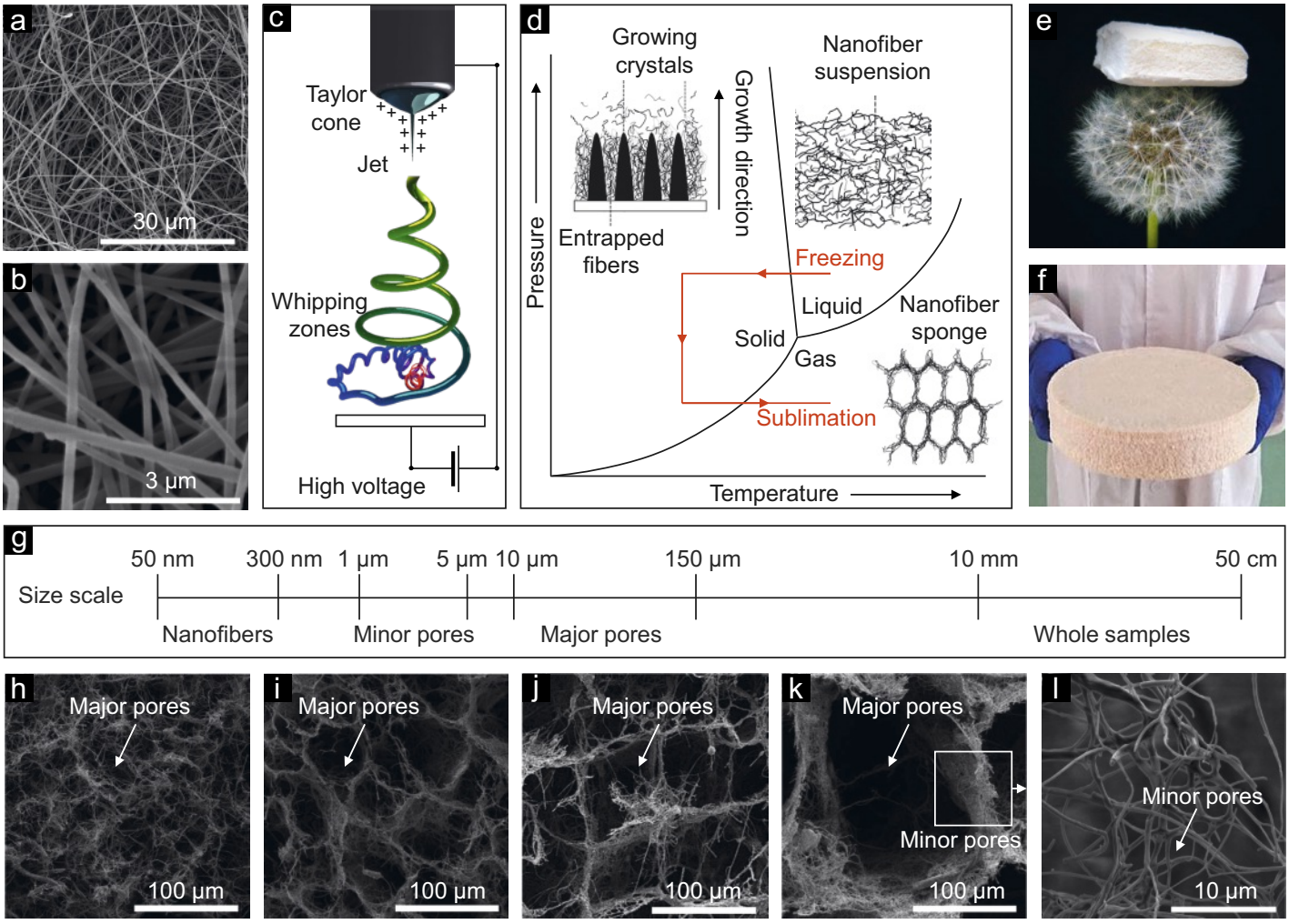

Fig. 2. Formation, properties and architecture of nanofiber sponges: (a,b) scanning electron microscope images of electrospun pullulan (Pul)/PVA nanofibers; (c) electrospinning process; (d) freeze-drying process with phase diagram; (e) ultra-light Pul/PVA nanofiber sponge supported from a dandelion (reproduced with permission from ref. [3a], © 2017 Chimia); (f) large-scale ion exchange nanofiber sponge (reproduced with permission from ref. [10], © 2018 John Wiley and Sons); (g) scale of hierarchical sponge architecture; (h-k) cellular major pores with tunable pore size (reproduced with permission from ref. [9], © 2016 BY-NC-ND 4.0) and (l) minor pores found in their cell walls.

where V is the volume of filtrate and t is the filtration time. The constant k_n and the exponent n characterize the filtration type with $n = 0$ for cake filtration, $n = 1$ for intermediate blocking, $n = 3/2$ for standard blocking and $n = 2$ for complete blocking (Fig. 3c).[28] The filter medium plays a crucial role in this process. Recently, it was shown that standard blocking occurred when yeast cell suspensions were filtered with a PA6-based nanofiber sponge while the pore volume was gradually filled by yeast cells deposited on the pore walls.[28] In contrast, the essentially 2D mat filter composed of nanofibers made of the same PA6 nanofibers functioned like a cake filter. The mean flux for the PA6 nanofiber sponge ranged from 2.5×10^3 to 7.5×10^3 l m^{-2} h^{-1} at >99% clarification, depending on the pore size (Table 3).[28] The mean flux for the 2D nanofiber mat was only 110 l m^{-2} h^{-1}.

Microplastic particles are considered emerging pollutants to the oceans and other ecosystems.[29] Therefore, we developed an efficient nanofiber sponge filter based on marine biomass.[30] When the chitosan nanofiber sponge was used as a conventional hydrostatic depth filter, PET microplastics were removed with an efficiency of 99.5% and a flux of 2.7×10^5 l m^{-2} h^{-1}. Due to its flexibility, the filter also allowed an alternative mode of operation, similar to oysters. Like an oyster, the sponge sat at the bottom of a tank and pumped a microplastic suspension through its pores through repeated cycles of pressure and release. After 4000 cycles, 80% of the microplastic had been removed from the basin and collected by the sponge.[30] While this was less efficient than using the sponge as a depth filter, the example shows how inherent properties of nanofiber sponges, such as their flexibility, allow for completely different and versatile modes of operation. Unlike for emulsions, the regeneration of filters with their entrapped particles after suspension filtration has not yet been studied.

Filtration of Solutions

To purify solutions by filtration, their solutes must interact with the stationary phase of the filtration column. This porous matrix can be a polymer monoblock, a gel, packed spheres, or a nanofiber sponge. Nanofiber sponges are attractive because their high porosity allows easy mass transfer at low differential pressure. At the same time, nanofibers offer great potential for tailored surface modifications to enable specific interactions such as electrostatic or ionic interactions (Fig. 3d). Recent examples include ion-exchange media developed by Fu *et al.* used in the field of bioseparation (Table 4).[10,31] Surface modification of SiO_2 nanofibers with PVA, citric acid, and polyphosphoric acid resulted in a highly carboxylated sponge with excellent adsorption capacity for the positively charged protein lysozyme.[10] Fu *et al.* demonstrated application of this sponge in a column for gravity-driven separation of lysozyme from egg white. The reported flux was high (1.6×10^4 l m^{-2} h^{-1}) and the adsorption capacity q_e was an impressive 2.9×10^3 mg g^{-1}. Regeneration was achieved by washing with PBS buffer. The adsorption dynamics could be further improved by switching to ethylene-vinyl alcohol copolymers (EVOH) and sur-

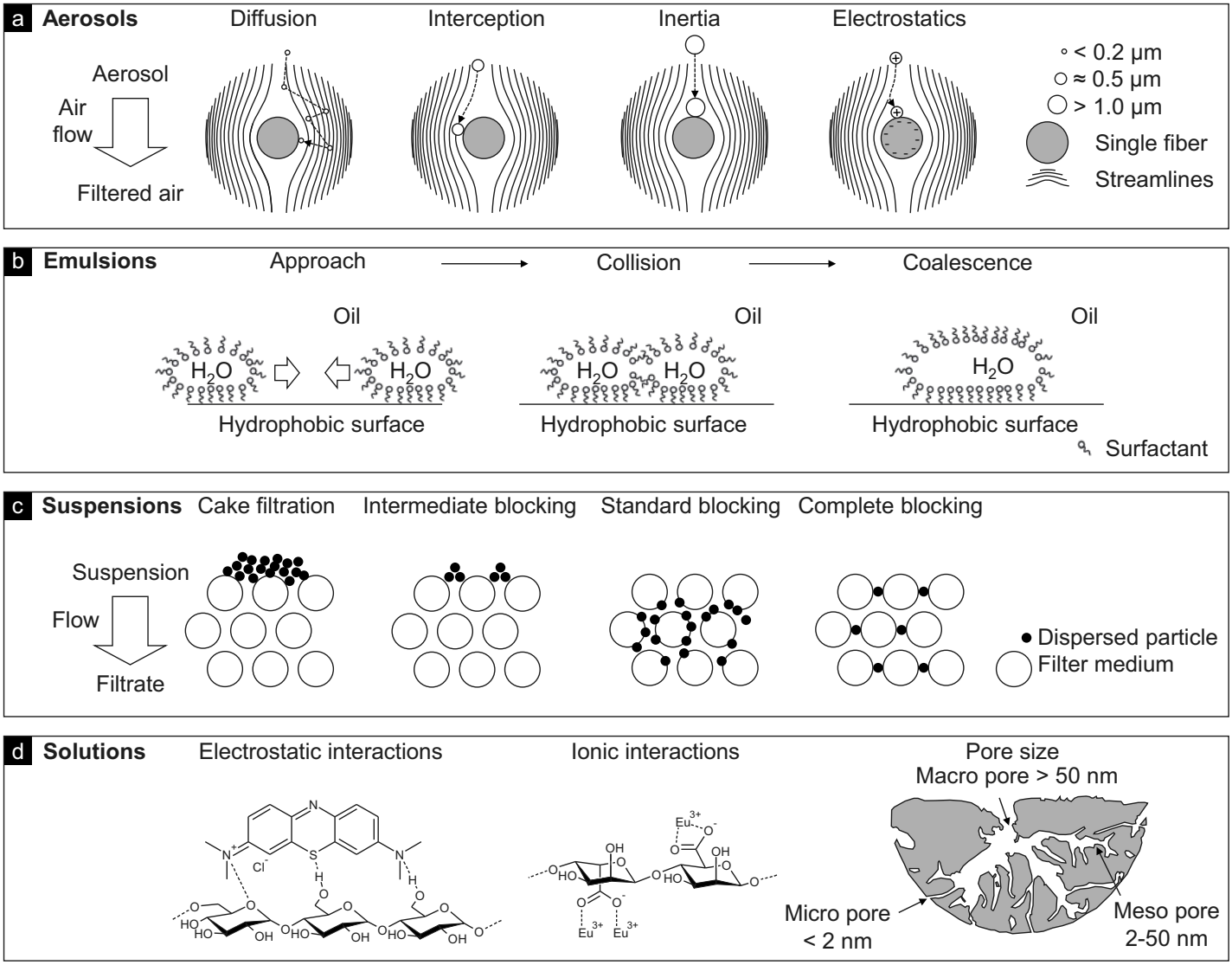

Fig. 3. Separation mechanisms for different mixtures: (a) aerosols; (b) emulsions; (c) suspensions and (d) solutions.

Table 1. Aerosol filtration using nanofiber sponges.

Fiber material	Application	Face velocity / cm^{-1}	Pressure drop / Pa	Efficiency / %
PI[a][16a]	$PM_{2.5}$[g]	18	177	99.9
PI[a][7]	$PM_{2.5}$[g]	7.1	240	99.83
PI/PTFE-PAI[ab][16b]	$PM_{0.3–10.0}$[g]	–	440	≥97.35
PI[7]	$PM_{0.3–10.0}$[g]	39.2	100	>60
PAI/BMI/SiO_2[ac][6]	$PM_{0.3}$[g]	5.3	211	99.982
PVA-*co*-PE[d][17]	NaCl	–	156	99.99
PAN[e][13]	$PM_{0.1}$[g]	10	54	99.72
Pul/PVA[f][5,9]	DEHS[h] 0.05–1.0 µm	1.5	550	99.998
Cellulose[20]	$PM_{0.3–10.0}$[g]	5.3	104	≥97.96
Cellulose/SiO_2[19a]	NaCl 0.3 µm	–	189	>99.97
Cellulose/lignin[19b]	DEHS[h] 0.1–1.0 µm	5	59.5	>99.6
Silk fibroin[18]	NaCl 0.24 µm	–	–	–

[a]Polyimide (PI); [b]polytetrafluoroethylene (PTFE)-polyamideimide (PAI); [c]bismaleimide (BMI); [d]poly(vinyl alcohol-co-ethylene) (PVA-co-PE); [e]polyacrylonitrile (PAN); [f]pullulan (Pul)/poly(vinyl alcohol) (PVA); [g]particulate matter (PM); [h]bis(2-ethylhexyl) sebacate (DEHS).

Table 2. Emulsion filtration using nanofiber sponges.

Fiber material	Functionalization	Application (cycles)	Flux / l m^{-2} h^{-1}	Efficiency / %
PAN/SiO_2[a][22]	SiO_2 NP[c] / bisphenol-AF	W/O (10)	≈ 1200	99.995
PI[b][24]	Silane	W/O (15)	1.8×10^5	94–99.5
Cellulose/alginate[25]	–	Oil/sea water (40)	1.7×10^4	97–99.65
Cellulose[27]	SiO_2 NP / silane	W/O (–)	6840	>98
Phenolic resin[26]	Hydrothermal	O/W and W/O (10)	250	99.9

[a]Polyacrylonitrile (PAN); [b]polyimide (PI); [c]nanoparticle (NP).

Table 3. Suspension filtration using nanofiber sponges. Polyamide 6 (PA6).

Fiber material	Functionalization	Application (cycles)	Flux / l m^{-2} h^{-1}	Efficiency / %
PA6[28]	-	Yeast cells (–)	2460–7500	99.5
Chitosan[30]	-	Microplastic (–)	2.7×10^5	> 99

face modification with polyphosphoric acid.[31] The importance of electrostatic interactions for the separation process was demonstrated using proteins with different isoelectric points. While bromelain and papain were adsorbed almost as well as lysozyme, the sponge was unable to adsorb negatively charged proteins such as BSA, ovalbumin or pepsin.[31]

A positively charged molecule, the dye methylene blue (MB), also served as a reference adsorbent for several sponges made of PVA silica modified with 2,5-dibromoaniline[32] or Pul/PVA/PAA (q_e = 383 mg g^{-1}[33]). The material was successfully used in a separation column and in batch adsorption experiments. The kinetics of the batch experiments were improved by mechanical compression and release, similar to the microplastic filter mentioned earlier.[30] Adsorption of the cationic MB was strongly pH dependent and washing with acidic solution (pH 3) allowed regeneration for 20 cycles. Other cations studied were the rare earths Tb^{3+} and Eu^{3+}, which adsorbed well on a sodium alginate/polyacrylamide sponge crosslinked with pyromellitic dianhydride (PMDA) (q_e = 498 mg g^{-1}).[34] The photoluminescent properties of the adsorbed Ln^{3+} sponge could be tuned by varying the Tb^{3+}/Eu^{3+} ratio between green and red emission.

Adsorption is not limited to positively charged solutes: a PAN/PEI sponge crosslinked with epichlorohydrin adsorbed both the anionic dye methyl orange, Cr(VI) and As(V) anions, and Cu(II) cations (q_e = 183-258 mg g^{-1}[35]). As expected, the adsorption capacity for Cu(II) cations increased with pH (pH 2 to 5), while it decreased for Cr(VI) (pH 2 to 10) and As(IV) anions (pH 2 to 8).

In general, adsorption properties are not only controlled by electrostatic interactions, but factors such as pore size, pore volume and specific surface area (Fig. 3d) are equally important – especially in the case of activated carbon, zeolites or metal-organic frameworks. Surprisingly, these materials have not yet been used in the context of nanofiber sponges.

Two-phase Systems

Oil spills and organic solvent leakage are easily treated by nanofiber sponges with tuned surface wettability.[3e] Hydrophobic and oleophilic surfaces with water contact angles between 136° and 162° were obtained by thermal treatment,[36] PPX or silane coating by chemical vapor deposition,[8,37] or deposition of SiO_2 nanoparticles.[22] The sponges prepared in this way adsorbed the organic phase within seconds due to their capillary forces until the entire cavity of the porous materials was filled with the organic phase.[37] Examples include diesel oil, gasoline, chloroform, hexane, or silicone oil, to name a few. The capacity was limited solely by the porosity and density of the liquids and ranged from 45 to 300 g g^{-1} (Table 5). The sponges could be successfully regenerated either by squeezing or evaporation, making these materials environmentally friendly mate-

Table 4. Solution purification using nanofiber sponges.

Fiber material	Functionalization	Application (cycles)	Flux / l m^{-2} h^{-1}	Capacity / mg g^{-1}
SiO_2[10]	PVA/CA/PPA[e]	Proteins (5)	1.56×10^4	2900
SiO_2[31]	EVOH/PPA[f]	Proteins (5)	1.50×10^4	3300
PVASi[a][32]	amine	MB[g] (5)	–	–
Pul/PVA/PAA[b][33]	–	MB[g] (20)	–	383
SA/PAM[c][34]	–	Eu^{3+}, Tb^{3+} (6)	–	498
PAN/PEI[d][35]	–	Cu(II), Cr(VI), As(V), MO[h] (7)		183–258

[a]crosslinked poly(vinyl alcohol) (PVA)/ tetraethyl orthosilicate (TEOS); [b]pullulan (Pul)/PVA/poly(acrylic acid) (PAA); [c]sodium alginate (SA)/polyacrylamide (PAM); [d]polyacrylonitrile (PAN)/polyethylenimine (PEI); [e]PVA/citric acid (CA)/poly(phosphoric acid) (PPA); [f]ethylene-vinyl alcohol copolymers (EVOH); [g]methylene blue (MB); [h]methyl orange (MO).

Table 5. Separation of two-phase systems using nanofiber sponges.

Fiber material	Functionalization	Application (cycles)	WCA[g] / °	Capacity / g g^{-1}
EVOH[a][38]	GA[d] crosslinking	Organics from water (10)	144.4	45–102
PAN/poly(MA-*co*-MMA-MABP)[b][8,39]	PPX[e]	Organics from water (5)	156	50–300
Cellulose[36]	PVA, thermal	Organics from water (10)	141	93–232
Pul/PVA[c][37]	TOS[f]	Organics from water (10)	136	50–117

[a]Ethylene-vinyl alcohol copolymers (EVOH); [b]polyacrylonitrile (PAN), methyl acrylate (MA), methyl methacrylate (MMA), 4-methacryloyloxybenzophenone (MABP); [c]pullulan/poly(vinyl alcohol) (PVA); [d]glutaraldehyde (GA); [e]poly(p-xylylene) (PPX); [f]trichloro(octyl) silane (TOS); [g]water contact angle (WCA).

rials for the separation of organic compounds from aqueous systems.[3e]

Conclusion and Outlook

Filtration will remain an important step in many industrial and environmental processes. Only eight years after their first mention, nanofiber sponges are proving to be excellent filters and adsorbers for a whole range of separation problems. They are often superior to existing filters made of nanofiber membranes or nanofiber mats. In particular, their large capacity should support early commercial use in areas where long maintenance intervals are economically relevant. To achieve widespread use, nanofiber starting materials and nanofiber sponge end products would need to become commercially available on a large scale. Alternatives to electrospinning, such as centrifugal spinning, are already being developed in the fiber manufacturing field. The current freeze-drying process for producing nanofiber sponges is versatile, *e.g.* in terms of controlling pore structure, but also slow. Advances in this area could drive the application of nanofiber sponges.

So where is the research going? To date, the versatility of nanofibers in terms of materials, functionalization, and loading has been exploited only to a limited extent for improved properties of nanofiber sponges. Molecularly imprinted polymers (MIPs) could control selectivity during adsorption, metal-organic frameworks (MOFs) could be used as selective adsorbents in CO_2 recovery, or catalytic purification processes are conceivable. As an alternative to the usual spherical particles used in analytical columns, nanofiber sponges could also become an interesting material.

Acknowledgements

The authors acknowledge the financial support through the Biomat@N grant of the Department of Life Sciences and Facility Management, ZHAW. P.R. acknowledges DSM Nutritional Products Ltd. and the Swiss Chemical Society for the Best Poster Presentation Award in Polymers, Colloids & Interfaces.

Received: January 31, 2022

[1] A. Rushton, A. S. Ward, R. G. Hodich, 'Solid-Liquid Filtration and Separation Technology', VCH Verlagsgesellschaft mbH, Weinheim, **1996**.
[2] M. Dilamian, M. Joghataei, Z. Ashrafi, C. Bohr, S. Mathur, H. Maleki, *Appl. Mater. Today* **2021**, *22*, https://doi.org/10.1016/j.apmt.2021.100964.
[3] a) F. Deuber, C. Adlhart, *Chimia* **2017**, *71*, 236, https://doi.org/10.2533/chimia.2017.236; b) S. Jiang, S. Agarwal, A. Greiner, *Angew. Chem. Int. Ed. Engl*. **2017**, *56*, 15520, https://doi.org/10.1002/anie.201700684; c) Z. Qian, Z. Wang, N. Zhao, J. Xu, Macromol. *Rapid Commun*. **2018**, *39*, e1700724, https://doi.org/10.1002/marc.201700724; d) Y. Chen, M. Shafiq, M. Liu, Y. Morsi, X. Mo, *Bioact. Mater*. **2020**, *5*, 963, https://doi.org/10.1016/j.bioactmat.2020.06.023; e) T. Xu, Y. Ding, Z. Liang, H. Sun, F. Zheng, Z. Zhu, Y. Zhao, H. Fong, *Prog. Mater. Sci.* **2020**, *112*, https://doi.org/10.1016/j.pmatsci.2020.100656.
[4] S. Jiang, G. Duan, U. Kuhn, M. Morl, V. Altstadt, A. L. Yarin, A. Greiner, *Angew. Chem. Int. Ed. Engl*. **2017**, *56*, 3285, https://doi.org/10.1002/anie.201611787.
[5] F. Deuber, S. Mousavi, L. Federer, M. Hofer, C. Adlhart, *ACS Appl. Mater. Interfaces* **2018**, *10*, 9069, https://doi.org/10.1021/acsami.8b00455.
[6] Y. Li, L. Cao, X. Yin, Y. Si, J. Yu, B. Ding, *Adv. Funct. Mater*. **2020**, *30*, https://doi.org/10.1002/adfm.201910426.
[7] Y. Shen, D. Li, B. Deng, Q. Liu, H. Liu, T. Wu, *R. Soc. Open Sci*. **2019**, *6*, 190596, https://doi.org/10.1098/rsos.190596.
[8] G. Duan, S. Jiang, T. Moss, S. Agarwal, A. Greiner, *Polym. Chem*. **2016**, *7*, 2759, https://doi.org/10.1039/c6py00339g.
[9] F. Deuber, S. Mousavi, M. Hofer, C. Adlhart, *Chemistry Select* **2016**, *1*, 5595, https://doi.org/10.1002/slct.201601084.
[10] Q. Fu, Y. Si, C. Duan, Z. Yan, L. Liu, J. Yu, B. Ding, *Adv. Funct. Mater*. **2019**, *29*, https://doi.org/10.1002/adfm.201808234.
[11] K. R. Spurny, 'Advances in Aerosol Filtration', CRC Press, Boca Raton, **1998**.
[12] European Standard EN 149:2001+A1:2009 D.
[13] Y. Zhang, Z. Zeng, X. Y. D. Ma, C. Zhao, J. M. Ang, B. F. Ng, M. P. Wan, S.-C. Wong, Z. Wang, X. Lu, *Appl. Surf. Sci*. **2019**, *479*, 700, https://doi.org/10.1016/j.apsusc.2019.02.173.
[14] S. Qiao, S. Kang, J. Zhu, Y. Wang, J. Yu, Z. Hu, *J. Hazard Mater.* **2021**, *415*, 125739, https://doi.org/10.1016/j.jhazmat.2021.125739.
[15] C. W. Hau, W. W. Leung, *Sep. Purif. Technol*. **2016**, *163*, 30, https://doi.org/10.1016/j.seppur.2016.02.041.
[16] a) Z. Qian, Z. Wang, Y. Chen, S. Tong, M. Ge, N. Zhao, J. Xu, *J. Mater. Chem. A* **2018**, *6*, 828, https://doi.org/10.1039/c7ta09054d; b) D. Li, H. Liu, Y. Shen, H. Wu, F. Liu, L. Wang, Q. Liu, B. Deng, *Nanomaterials* **2020**, *10*, https://doi.org/10.3390/nano10091806.
[17] Q. Liu, J. Chen, T. Mei, X. He, W. Zhong, K. Liu, W. Wang, Y. Wang, M. Li, D. Wang, *J. Mater. Chem. A* **2018**, *6*, 3692, https://doi.org/10.1039/c7ta10107d.
[18] X. Xie, Z. Zheng, X. Wang, D. Lee Kaplan, *ACS Nano* **2021**, *15*, 1048, https://doi.org/10.1021/acsnano.0c07896.
[19] a) F. Wang, Y. Si, J. Yu, B. Ding, *Adv. Funct. Mater*. **2021**, *31*, https://doi.org/10.1002/adfm.202107223; b) X. Y. D. Ma, Z. Zeng, Z. Wang, L. Xu, Y. Zhang, J. M. Ang, M. P. Wan, B. F. Ng, X. Lu, *J. Membr. Sci*. **2022**, *642*, https://doi.org/10.1016/j.memsci.2021.119977.
[20] T. Liu, C. Cai, R. Ma, Y. Deng, L. Tu, Y. Fan, D. Lu, *ACS Appl Mater Interfaces* **2021**, *13*, 24032, https://doi.org/10.1021/acsami.1c04258.
[21] N. M. Kocherginsky, C. L. Tan, W. F. Lu, *J. Membr. Sci*. **2003**, *220*, 117, https://doi.org/10.1016/s0376-7388(03)00223-0.
[22] Y. Si, Q. Fu, X. Wang, J. Zhu, J. Yu, G. Sun, B. Ding, *ACS Nano* **2015**, *9*, 3791, https://doi.org/10.1021/nn506633b.
[23] Q. Zhang, L. Li, L. Cao, Y. Li, W. Li, *Chin. J. Chem. Eng*. **2021**, *36*, 29, https://doi.org/10.1016/j.cjche.2020.07.034.
[24] Y. Shen, D. Li, L. Wang, Y. Zhou, F. Liu, H. Wu, B. Deng, Q. Liu, *ACS Appl. Mater. Interfaces* **2021**, *13*, 20489, https://doi.org/10.1021/acsami.1c01136.
[25] Y. Li, H. Zhang, M. Fan, J. Zhuang, L. Chen, *Phys. Chem. Chem. Phys*. **2016**, *18*, 25394, https://doi.org/10.1039/c6cp04284h.
[26] X. Li, L. You, Y. Song, L. Gao, Y. Liu, W. Chen, L. Mao, *Langmuir* **2019**, *35*, 14902, https://doi.org/10.1021/acs.langmuir.9b02750.
[27] S. Zhou, T. You, X. Zhang, F. Xu, *ACS Appl Nano Mater*. **2018**, *1*, 2095, https://doi.org/10.1021/acsanm.8b00079.

[28] S. Mousavi, L. Filipová, J. Ebert, F. J. Heiligtag, R. Daumke, W. Loser, B. Ledergerber, B. Frank, C. Adlhart, *Sep. Purif. Technol*. **2022**, *284*, https://doi.org/10.1016/j.seppur.2021.120273.
[29] F. Zhang, Y. B. Man, W. Y. Mo, K. Y. Man, M. H. Wong, *Crit. Rev. Environ. Sci. Technol*. **2020**, *50*, 2109, https://doi.org/10.1080/10643389.2019.1700752.
[30] P. Risch, C. Adlhart, *ACS Appl. Nano Mater*. **2021**, *3*, 4685, https://doi.org/10.1021/acsapm.1c00799.
[31] Q. Fu, L. Liu, Y. Si, J. Yu, B. Ding, *ACS Appl. Mater. Interfaces* **2019**, *11*, 44874, https://doi.org/10.1021/acsami.9b15760.
[32] J. G. Kim, T. J. Choi, J. Y. Chang, *Chem. Eng. J*. **2016**, *306*, 242, https://doi.org/10.1016/j.cej.2016.07.055.
[33] S. Mousavi, F. Deuber, S. Petrozzi, L. Federer, M. Aliabadi, F. Shahraki, C. Adlhart, *Colloids Surf., A* **2018**, *547*, 117, https://doi.org/10.1016/j.colsurfa.2018.03.052.
[34] M. Wang, X. Li, W. Hua, L. Deng, P. Li, T. Zhang, X. Wang, *Chem. Eng. J*. **2018**, *348*, 95, https://doi.org/10.1016/j.cej.2018.04.135.
[35] L. Xue, J. Ren, S. Wang, D. Qu, Z. Wei, Q. Yang, Y. Li, *J. Porous Mater*. **2020**, *27*, 1589, https://doi.org/10.1007/s10934-020-00937-6.
[36] T. Xu, Z. Wang, Y. Ding, W. Xu, W. Wu, Z. Zhu, H. Fong, *Carbohydr. Polym*. **2018**, *179*, 164, https://doi.org/10.1016/j.carbpol.2017.09.086.
[37] F. Deuber, S. Mousavi, L. Federer, C. Adlhart, *Adv. Mater. Interfaces* **2017**, *4*, https://doi.org/10.1002/admi.201700065.
[38] J. Lu, D. Xu, J. Wei, S. Yan, R. Xiao, *ACS Appl. Mater. Interfaces* **2017**, *9*, 25533, https://doi.org/10.1021/acsami.7b07004.
[39] G. Duan, S. Jiang, V. Jérôme, J. H. Wendorff, A. Fathi, J. Uhm, V. Altstädt, M. Herling, J. Breu, R. Freitag, S. Agarwal, A. Greiner, *Adv. Funct. Mater*. **2015**, *25*, 2850, https://doi.org/10.1002/adfm.201500001.

License and Terms

The definitive version of this article is the electronic one that can be found at https://doi.org/10.2533/chimia.2022.354